Three-Dimensional Conduction Effects During Scribing with a CW Laser

Subhransu Roy* and Michael F. Modest†
The Pennsylvania State University, University Park, Pennsylvania

A three-dimensional conduction model has been developed to predict the shape of the groove formed by partially evaporating the surface of a semi-infinite body using a moving Gaussian laser beam. The full three-dimensional conduction equation with relevant nonlinear boundary conditions is solved using the boundary-element method, and results for groove depth and shape are compared for a variety of laser and solid parameters with a one-dimensional conduction model where conduction losses were treated in an approximate fashion using a simple integral method. As expected, it is observed that when thermal losses due to conduction are minor, the approximate one-dimensional conduction solution is very close to the three-dimensional solution (large laser scanning speeds, low thermal conductivity). The three-dimensional model is always able to predict the correct smooth groove shape along the centerplane $\eta = 0$. This cannot be predicted by the one-dimensional conduction model because of the neglected sideways conduction, leading to serious errors in the prediction of maximum groove depths.

Nomenclature

c	= specific heat [kJ/kg K]
F_0	= radiation flux density at center of beam, [W/m^2]
h_{ig}	= heat of removal, [kJ/kg]
H	= irradiation flux vector, [W/m^2]
$\hat{\imath},\hat{k}$	= unit vector in x *and* z directions
k	= thermal conductivity [Wm/K]
$[M]$	= shape function matrix
$\hat{n}$	= outward unit surface normal
N	= total number of boundary elements
N_e	= evaporation-to-laser power parameter
N_k	= conduction-to-laser power parameter
$\bar{q}$	= nondimensionalized temperature gradient at surface
Q	= nondimensionalized irradiation flux vector at surface
$\hat{r}_i$	= unit vector from node i to (ξ,η,ζ)
R_0	= effective radius of laser beam [m]
s, S	= groove depth [m, $-$]
s_∞,S_∞	= fully developed groove shape [m, $-$]
T_{ev}	= evaporation temperature [K]
T_∞	= ambient temperature [K]
u	= laser scanning speed [m/s]
U	= laser speed-to-diffusion parameter
x,y,z	= Cartesian coordinates
x_1,x_2	= local coordinates for the element
$\alpha(x,y)$	= local effective absorptivity at laser wavelength
α_0	= reference absorptivity
Γ_g,Γ_∞	= boundary surface of medium [m^2]
θ	= nondimensionalized temperature
$\bar{\theta}$	= nondimensionalized surface temperature
ξ,η,ζ	= nondimensionalized x,y,z coordinates
ρ	= density of the medium [kg/m^3]
ω_i	= interior solid angle at node point i [sr]
Ω	= volume of medium [m^3]

Presented as Paper 89-0179 at the AIAA 27th Aerospace Sciences Meeting, Reno, NV, Jan. 9–12, 1989; received Feb. 2, 1989; revision received May 24, 1989.

*Research Assistant, Department of Mechanical Engineering.

†Professor, Department of Mechanical Engineering. Member AIAA.

Introduction

LASERS have a variety of applications in modern technology because of their ability to produce high-power beams. Laser applications include welding, drilling, cutting, scribing, machining, heat treatment, and medical surgery, among others.

Most of the theoretical work on laser-processing heat transfer to date has centered on the solution of the classical heat-conduction equation for a stationary or moving semi-infinite solid. Cases with and without phase change and for a variety of irradiation conditions have been studied. The simplest case without phase change, where a body is heated uniformly over its entire boundary surface, was first treated by Carslaw and Jaeger,[1] and a pulsed heat source was addressed by Carslaw and Jaeger,[1] White,[2,3] and Rykalin et al.[4] A disk-shaped source was first treated by Paek and Gagliano,[5] and a Gaussian power distribution was investigated by Ready.[6] The case of a semitransparent solid was first addressed by Brugger[7] and Maydan[8,9] for the one-dimensional conduction case. The most general heat-conduction solution is given by Modest and Abakians,[10] who looked at a moving semitransparent body irradiated by a Gaussian laser source either uniformly in time or in pulsed mode.

The problem is considerably more complicated when phase change takes place. Soodak[11] was the first to study the problem of melting with complete removal of melt for a one-dimensional slab. Landau[12] considered the same problem for the case that one surface was subjected to time-varying heating. Dabby and Paek[13] considered laser penetration into the solid for a stationary semi-infinite solid. To model the laser drilling process, von Allmen[14] found a quasi-one-dimensional solution that showed considerable agreement with experiments. Laser scribing or shaping with a moving laser was first modeled by Modest and Abakians[15] for irradiation by a continuous-wave (CW) laser with Gaussian distribution onto an opaque semi-infinite solid. They assumed one-step evaporation of material (without beam interference), parallel laser beams, negligible reflection effects, and small heat losses (in order to employ a simple integral method for conduction losses). The use of the integral profile technique for moving boundary problems was pioneered by Goodman[16] and has found widespread application to a variety of melting and solidification processes. The assumption of a parallel laser beam was relaxed by Biyikli and Modest,[17] who investigated the effects of beam focusing and focal plane position. In another follow-up paper by Abakians and Modest,[18] semitransparent bodies were considered, showing that materials would have to be very transparent to display substantially different behavior. In the present paper, one of the weakest assumptions made by Modest et al.[15,17,18] will be relaxed: rather than treating conduction losses in a quasi-one-dimensional fashion, the full three-dimensional conduction equation will be solved. The results show that a more accurate treatment of the conduction losses has a considerable effect on the size of the groove formed by evaporation even if scanning velocity is fairly high (resulting in small conduction losses). For many metals and ceramic materials the thermal diffusivity is high enough to make the ratio of scanning speed to that of thermal diffusivity (described later as U) low. For such materials three-dimensional conduction effects must be included to predict a realistic groove depth.

Theoretical Background

In order to obtain a realistic yet feasible description of the evaporation front in a moving solid subjected to a concentrated laser beam, the following simplifying assumptions will be made:

1) The solid moves with constant velocity u, and the frame of reference is fixed to the laser.

2) The solid is isotropic with constant properties. Since the main emphasis of the present work is to study the effect of three-dimensional conduction compared to the one-dimensional conduction model,[15,17,18] this assumption is made for mathematical simplification. Property variations will be incorporated in a later study.

3) The material is opaque; i.e., the laser beam does not penetrate appreciably into the medium. It was shown by Abakians and Modest[18] that the absorption coefficient would have to be very small to make this a poor assumption.

4) Change of phase from solid to vapor occurs in a single step at the T_{ev}. Real materials may display significantly different behavior,[15,18] such as liquefaction followed by evaporation, decomposition into liquid and gas, gradual evaporation over a wide range of temperatures, outgassing followed by microexplosive removal of solid particles, etc. Assuming that the most important parameter is the total amount of energy required to remove material, referred to as heat of removal, h_{ig}, the present model should do quite well.

5) The evaporated material does not interfere with the incoming laser beam: most CW laser processing takes place at moderate power levels (i.e., without substantial plasma formation), keeping the gas above the workpiece transparent. We also assume that there are no droplets and particles (or they are removed by an external gas jet).

6) Heat losses by convection and radiation are negligible (compared to conduction and change-of-phase losses). This was shown by Modest and Abakians[15] to be accurate under all conditions.

7) Multiple reflections of laser radiation within the groove are neglected. This is a limitation that restricts the present model to shallow grooves or materials with high absorptivities (even at grazing angles), e.g., if the evaporation surface is rough.

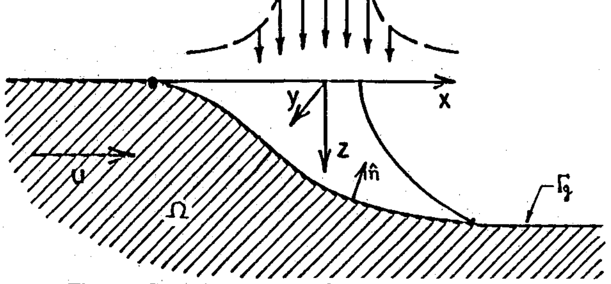

Fig. 1 Coordinate system for groove formation.

Under these conditions the heat-transfer problem in the semi-infinite region Ω, bounded by Γ_∞ at infinity and Γ_g at the grooved surface, with the coordinate system fixed to the laser position, is governed by the quasi-steady three-dimensional conduction equation for a moving body[1,15] (cf. Fig. 1):

$$U\frac{\partial\theta}{\partial\xi} = \frac{\partial^2\theta}{\partial\xi^2} + \frac{\partial^2\theta}{\partial\eta^2} + \frac{\partial^2\theta}{\partial\zeta^2} \quad \text{in } \Omega \tag{1}$$

$$\xi \rightarrow \pm\infty, \quad \eta \rightarrow \pm\infty, \quad \zeta \rightarrow +\infty: \quad \bar{\theta} = 0; \quad \text{on} \quad \Gamma_\infty \tag{2}$$

$$\zeta = S(\xi,\eta): \quad \bar{q} = \hat{n}\cdot\nabla\theta = -\frac{1}{N_k}Q(\xi,\eta)\cdot\hat{n} - \frac{N_e}{N_k}(\hat{\imath}\cdot\hat{n}) \text{ on } \Gamma_g \tag{3a}$$

$$\theta(\xi,\eta) = 1 \qquad \text{if } \hat{\imath}\cdot\hat{n} > 0 \tag{3b}$$

where the following nondimensional variables and parameters have been introduced[15]:

$$\xi = x/R_0, \qquad \eta = y/R_0, \qquad \zeta = z/R_0 \tag{4a}$$

$$S = \frac{s(x,y)}{R_0}, \qquad \theta = \frac{(T - T_\infty)}{(T_{ev} - T_\infty)}, \qquad Q = \frac{\alpha(x,y)H(x,y)}{\alpha_0 F_0} \tag{4b}$$

$$N_e = \frac{\rho u h_{ig}}{\alpha_0 F_0}, \qquad N_k = \frac{k(T_{ev} - T_\infty)}{\alpha_0 F_0 R_0}, \qquad U = \frac{\rho c u R_0}{k} \tag{4c}$$

Physically, N_e gives the ratio of power required to evaporate material normal to the irradiation and absorbed laser flux. The N_k approximates the ratio of conduction losses, again for a surface normal to irradiation, and absorbed laser flux. Finally, U relates the laser scanning speed to that of thermal diffusion into the medium.

The laser beam is assumed to be parallel, although beam focusing[17] can be accommodated in the present computer code. Since the main emphasis of the present work is to study the effect of three-dimensional conduction, compared to the one-dimensional conduction model,[15,17,18] the assumption of a parallel beam is adopted for the sake of simplicity. For the present set of assumptions (i.e., parallel beam, no multiple reflections, constant absorptivity), the intensity of the laser beam on the surface of the groove is

$$Q = \frac{H(\xi,\eta)}{F_0} = e^{-(\xi^2+\eta^2)}\hat{k} \tag{5}$$

The boundary condition [Eq. (3a)] states that the absorbed irradiation is used up by conduction losses into the solid and by evaporation, if present (if no evaporation takes place, i.e., during warmup, cooldown, and in regions too far away sideways from the laser beam, then $\hat{\imath}\cdot\hat{n} = 0$), and Eq. (3b) states that during evaporation (i.e., when $\hat{\imath}\cdot\hat{n} > 0$) the surface is at evaporation temperature.

Equation (1) with its boundary conditions [Eq. (2–5)] form a complete set of equations for the solution of the temperature field θ. The additional boundary condition (3b) over the evaporation region is required for the determination of the groove depth S. This set of equations is similar to the one used by Modest et al.,[15,17,18] except that the full three-dimensional conduction equation (1) will be solved here (rather than using a one-dimensional integral method).

Solution Approach

Equation (1) with boundary conditions in Eqs. (2) and (3) is solved by the boundary-element method (BEM). The BEM is a technique based on the combination of classical integral equations and finite-element concepts.[19,20] In this solution method, the boundary is divided into elements and the nodes are defined only on the boundary of the domain; internal nodes need not be defined as the problem mathematically is reduced to a boundary solution problem. This reduction is possible by applying Green's theorem and using fundamental solutions that satisfy the governing equations or parts of them. An added advantage for semi-infinite media is that, since the BEM solution automatically satisfies admissible boundary conditions at infinity, no subdivisions of these boundaries arise. This method is particularly desirable for the present problem, since only the solution at the free boundary is needed. For the BEM solution, Eq. (1) is written in weighted residual form[19,20] by defining a distribution function T^* such that

$$\int_\Omega \left(\nabla^2\theta - U\frac{\partial\theta}{\partial\xi} \right) T^* \mathrm{d}\Omega = \int_{\Gamma_g} (q - \bar{q}) T^* \mathrm{d}\Gamma$$

$$- \int_{\Gamma_\infty} (\theta - \bar{\theta}) \frac{\partial T^*}{\partial n} \, \mathrm{d}\Gamma - \int_{\Gamma_\infty} U(\theta - \bar{\theta}) T^* (\hat{\imath} \cdot \hat{n}) \, \mathrm{d}\Gamma \tag{6a}$$

where $q = \partial\theta/\partial n$.

Integrating the Laplacian in the preceding expression twice by parts and $U(\partial\theta/\partial\xi)$ once, the following relationship is obtained:

$$\int_\Omega \left(\nabla^2 T^* + U\frac{\partial T^*}{\partial\xi} \right) \theta \, \mathrm{d}\Omega$$

$$= \int_{\Gamma_g} \left[-\bar{q}T^* + \theta\frac{\partial T^*}{\partial n} + U\theta T^*(\hat{\imath}\cdot\hat{n}) \right] \mathrm{d}\Gamma$$

$$+ \int_{\Gamma_\infty} \left[-qT^* + \bar{\theta}\frac{\partial T^*}{\partial n} + U\bar{\theta}T^*(\hat{\imath}\cdot\hat{n}) \right] \mathrm{d}\Gamma \tag{6b}$$

In order to eliminate the domain integral in Eq. (6b), the function T^* is assumed to be a fundamental solution (also called the Green's function) of the following equation:

$$\nabla^2 T^* + U\frac{\partial T^*}{\partial\xi} + \delta_i(R) = 0 \tag{6c}$$

$$R^2 = (\xi - \xi_i)^2 + (\eta - \eta_i)^2 + (\zeta - \zeta_i)^2 \tag{6d}$$

where $\delta_i(R)$ is the Dirac delta function, and R is the distance of any point (ξ,η,ζ) in Ω from a nodal point $(\xi_i,\eta_i,\zeta_i = S_i)$ on the boundary.

The Green's function for Eq. (6c) is[1]

$$T^* = \frac{1}{4\pi R}\exp\left[-\frac{U}{2}(R + \xi - \xi_i) \right] \tag{7}$$

Substituting Eqs. (6c) and (7) into Eq. (6b), one finds the following expression for a nodal point i on the boundary:

$$c_i\theta_i = \int_{\Gamma_g} \left[\bar{q}T^* - \theta\frac{\partial T^*}{\partial n} - U\theta T^*(\hat{\imath}\cdot\hat{n}) \right] \mathrm{d}\Gamma \tag{8}$$

The last integral in Eq. (6b) has disappeared since $T^* \to 0$ on Γ_∞. The factor c_i comes from the Γ_g^--integration of the term $(\partial T^*/\partial n)$ at nodal point i, where this term is singular; the contribution from the Γ_g-integration of the other singular terms in Eq. (8) containing T^* is zero. The surface integration over the singular point is performed by considering a spherical region, of radius $\epsilon \to 0$, enclosing node i.[20] This leads to $c_i = \omega_i/4\pi$, where ω_i is the interior solid angle subtended by the surface at node point i, e.g., $c_i = 1/2$ for a smooth surface. For a sharp corner or a curved surface made up of boundary elements of C^0 continuity (i.e., the function itself – zeroth derivative, but not higher-order derivatives – is continuous across interelement boundaries), $c_i \neq 1/2$ at the corner points. The integral in Eq. (8) in the vicinity of point i is to be evaluated in the Cauchy principal value sense. After substituting $\bar{q}$ from Eq. (3a) and evaluating $\partial T^*/\partial n$, Eq. (8) reduces to

$$c_i\theta_i + \int_{\Gamma_g} \left[\frac{U}{2}T^*\hat{\imath} - \left(\frac{U}{2} + \frac{1}{R} \right) T^*\hat{r}_i \right] \cdot \hat{n}\theta \, \mathrm{d}\Gamma$$

$$= -\int_{\Gamma_g} T^* \left(\frac{Q}{N_k} + \frac{N_e}{N_k}\hat{\imath} \right) \cdot \hat{n} \, \mathrm{d}\Gamma \tag{9a}$$

where $\hat{r}_i$ is a unit vector pointing from (ξ_i, η_i, S_i) to (ξ, η, S). This equation may be written in abbreviated form as

$$c_i\theta_i + \int_{\Gamma_g} F_i(\xi_i,\eta_i,S_i,\xi,\eta,S)\theta \, \mathrm{d}\Gamma$$

$$= \int_{\Gamma_g} G_i(\xi_i,\eta_i,S_i,\xi,\eta,S) \, \mathrm{d}\Gamma \tag{9b}$$

where F_i collects all of the terms in the first integral in Eq. (9a), and G_i collects those of the other. Care must be taken in the integration of Eqs. (9) in the vicinity of i because of the singularity in T^*.

To facilitate the solution of Eqs. (9), the region of interest (i.e., the groove and its vicinity) on the boundary surface Γ_g is divided into many triangular and quadrilateral elements having node points at each corner as depicted in Fig. 2. This region of interest is connected to the boundary Γ_∞, at infinity, by "infinite boundary elements" as proposed by Watson.[21] For computational efficiency, only half of the groove is divided into elements since, in the present case of a single groove, the groove is symmetric about the plane $\eta = 0$. The ξ,η,S coordinates and temperature θ on the groove surface are discretized in terms of the nodal values, using an isoparametric linear element representation[19,20]:

$$\xi = [M]_p\{\xi\}, \qquad \eta = [M]_p\{\eta\} \tag{10a}$$

$$S = [M]_p\{S\}, \qquad \theta = [M]_p\{\theta\} \tag{10b}$$

where $[M]_p$ is the shape function matrix for the linear element p, and the variable within { } is a column vector containing all nodal values for element p. For example, for the nondimen-

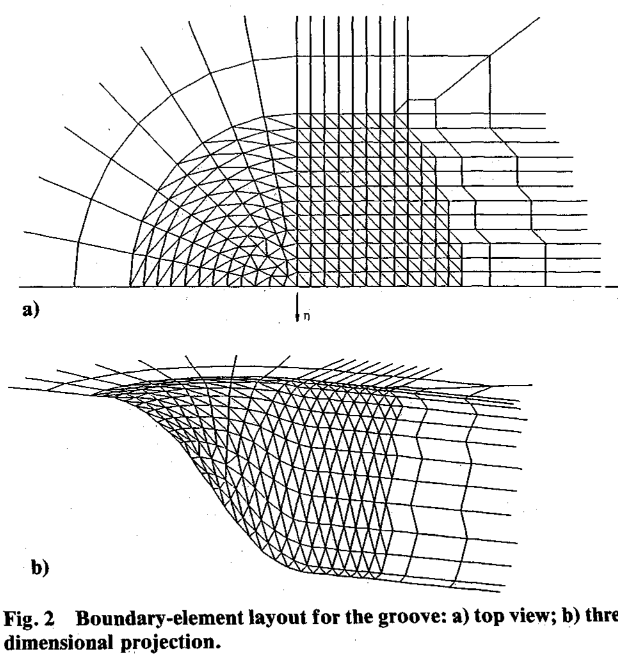

Fig. 2 Boundary-element layout for the groove: a) top view; b) three-dimensional projection.

sional temperature on a linear triangular element,

$$\theta = [x_1\ x_2\ (1 - x_1 - x_2)] \begin{Bmatrix} \theta_1 \\ \theta_2 \\ \theta_3 \end{Bmatrix} \tag{11}$$

where x_1 and x_2 are the local coordinates (cf. Fig. 3). Then the discretized form of Eqs. (9) for a number of N elements becomes

$$c_i\theta_i + \left(\sum_{p=1}^{N} \int_{\Gamma_p} F_i[M]_p \, d\Gamma \right) \{\theta\} = \sum_{p=1}^{N} \int_{\Gamma_p} G_i \, d\Gamma \tag{12}$$

The integral in Eq. (12) for each boundary element Γ_p is evaluated using a Gaussian quadrature. This results in a set of algebraic equations, one for each nodal point i. These equations are consolidated into matrix form:

$$[A]\{\theta\} = \{B\} \tag{13}$$

The resultant $[A]$ matrix is a full matrix, and the equation is solved by an IMSL routine that uses Gaussian elimination (Crout algorithm) and partial pivoting with final iterative refinement.

A first approximation of S (i.e., the groove shape) is obtained by using an integral method and by neglecting conduction parallel to the surface, as well as reflections; this makes the equations governing groove depth (S) first-order hyperbolic; thus, they can be solved with a simple forward-stepping technique.[15,17,18] For known values of S, new values of absorbed flux Q and temperature θ are calculated. Wherever $\theta > 1$, the value of S is increased, and wherever $\theta < 1$ while $\hat{\imath} \cdot \hat{n} > 0$, S is decreased until the surface temperature converges to $\theta = 1$. The incremental (or decremental) value for S is estimated as follows: an approximate linear temperature profile is estimated from Eq. (3a); then the material removed using the energy for temperature in excess of $\theta = 1$ is calculated from the known value of "heat of removal." However, S is only incremented (or decremented) by a fraction (0.5–0.8) of this estimated amount to obtain a stable solution. To insure numerical stability, it was also necessary to limit the maximum change in S to one-tenth of the grid size. The uniqueness property of BEM solutions has been an academic concern for quite some time. This code was run with some slightly different initial groove depths. It was observed that, if the depth increment is kept within the prescribed limits, converged solutions could be obtained.

Discussion of Results

Figure 4 shows how a typical groove develops along the ξ direction for the case of $U = 10$, $N_k = 0.01$, and $N_e = 0.1$. For $\xi > 0.4$–0.5 (the location where the groove achieves its maximum width), no additional evaporation beyond a certain η will occur, since part of the groove has moved too far away from the laser center; i.e., the entire amount of laser radiation is lost to conduction. For example, as depicted in Fig. 4 at $\xi = 0.51$, no more evaporation occurs beyond $\eta = 1.87$ (indicated by a circle). This point moves rapidly toward the center of the groove because of increasing heat losses (due to steepness of the groove wall) and reaches $\eta = 0.68$ at $\xi = 1.02$ (cf. Fig. 4). The difference between the one-dimensional and three-dimensional solutions at a particular ξ location decreases with larger η as the conduction losses become smaller, and both solutions are very close together at the periphery of the groove. Figure 5 shows the development of centerline groove depth for constant energy deposition per unit area, but at three different scanning speeds. It is observed that the three-dimensional model and one-dimensional conduction model predictions are very close for negative ξ locations (i.e., when the groove has just started forming) even at the centerline because of low conduction losses and since the one-dimensional conduction model correctly predicts $\partial S/\partial\eta = 0$ in this region. Because the BEM grid for $\xi < 0$ is radial as shown in Fig. 2, the full groove

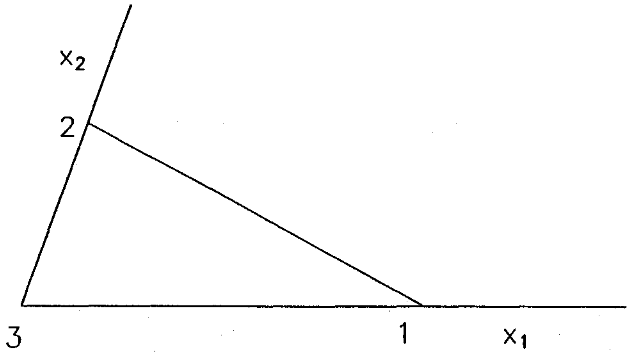

Fig. 3 Triangular boundary element.

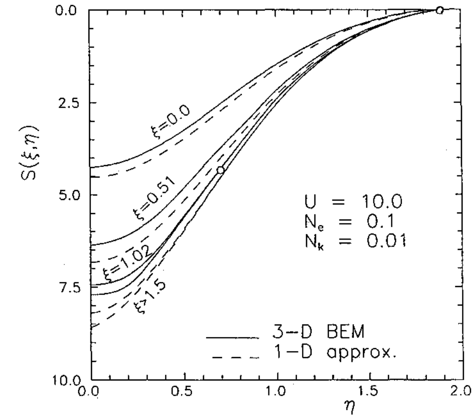

Fig. 4 Groove cross section at different ξ locations in the evaporating region.

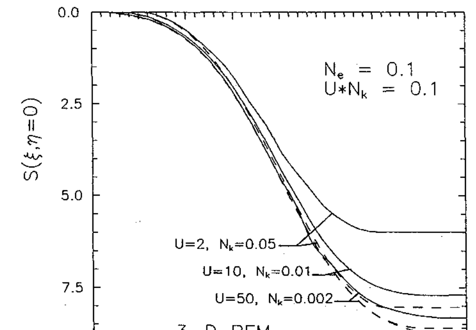

Fig. 5 Groove development along centerline.

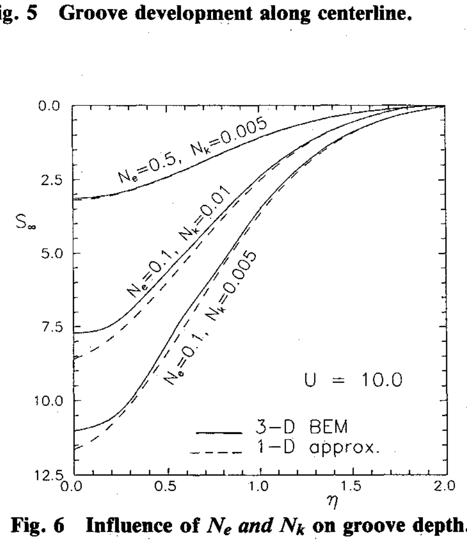

Fig. 6 Influence of N_e and N_k on groove depth.

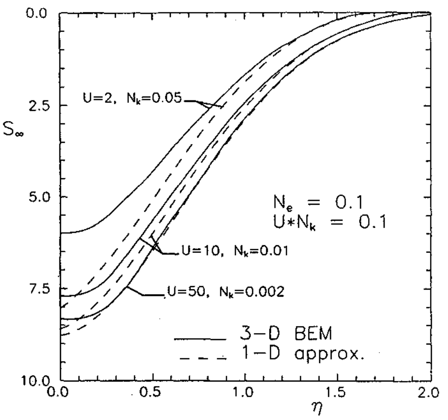

Fig. 7 Influence of scanning speed U on groove depth.

cross section at a particular negative ξ obtained from the three-dimensional solution could not be compared with the one-dimensional conduction solution. For positive ξ, the one-dimensional and three-dimensional models diverge more and more since the one-dimensional model, neglecting sideways conduction, predicts $\partial S/\partial\eta \neq 0$ at the centerline. This is particularly pronounced for slow scanning speeds, when conduction losses become more important.

The influence of the latent heat-to-laser power parameter N_e on the importance of three-dimensional conduction is shown in Fig. 6. Here $U=10$ and $N_k=0.005$ have been selected as representative values. Large values of N_e ($N_e=0.5$) generally mean shallow grooves and, therefore, relatively small heat losses (the ratio of groove surface to that normal to the laser beam is relatively small due to shallowness of the groove). A small N_e implies large laser power F_0, or a small "heat of removal" h_{ig}. The one-dimensional conduction model predicts groove shape well for relatively shallow grooves. For deeper grooves, conduction losses become more important (even for the same N_k) because of the larger surface area. Changes in the groove depth for different values of conduction loss parameter N_k are also shown in Fig. 6. For large values of N_k, the laser energy is mostly taken away by conductive losses, explaining the shallow groove and the poorer performance of the one-dimensional conduction model. It is also observed that the three-dimensional model is able to predict a realistic groove shape with $\partial S/\partial\eta=0$ at the centerline, which is not possible with the one-dimensional conduction model.

Figure 7 shows the effect of U, the ratio of laser scanning speed to that of heat diffusion into the medium, on the fully developed groove shape S_∞. As in Fig. 4, N_e is kept at a typical value of 0.1, and $U\times N_k$ is kept constant for all three cases, which ensures that the irradiated energy/unit area is identical. Thus, increasing U will decrease conduction losses, and the maximum groove depth will increase. Comparing the three-dimensional solution with the one-dimensional conduction solution, it is observed that for large U, as the conduction losses decrease, the approximate one-dimensional conduction solution predicts the groove very well except near the centerline.

Conclusions

A fully three-dimensional conduction model using the boundary element method (BEM) has been developed to predict the shape of a groove formed by partially evaporating the surface of a semi-infinite body using a moving Gaussian laser beam. It is observed that, for a moderately small conduction loss parameter ($N_k<0.01$) and $U\times N_k<0.1$ (i.e., moderate energy deposition/per unit area), the approximate one-dimensional conduction solution is very close to the three-dimensional solution. The three-dimensional model is always able to predict the correct smooth groove shape along the centerplane $\eta=0$, which cannot be predicted by the one-dimensional conduction model because of the neglected sideways conduction.

The range for which the simple one-dimensional conduction model gives good estimation of groove depth and shape has been established by comparing with the three-dimensional conduction model. The one-dimensional model is good for small conduction losses, i.e., large U ($U>10$) and small $S_{max}\times N_k$, say $S_{max}\times N_k<0.05$ (since N_k is a measure of conduction losses per unit groove area projected onto the $\zeta=0$ plane). The one-dimensional conduction model predictions are particularly poor at the centerline: the equations governing groove depth[15] (S) is first-order hyperbolic and one of the characteristic lines fall onto the centerline, allowing a discontinuity there. Therefore, the condition of $\partial S/\partial\eta=0$ is not enforced, and the one-dimensional model often predicts a sharp apex at $\eta=0$.

Acknowledgment

Support for this work by National Science Foundation Grant CBT-8711255 is gratefully acknowledged.

References

[1]Carslaw, H. S. and Jaeger, J. C., *Conduction of Heat in Solids*, 2nd ed., Oxford University Press, Oxford, UK, 1959.

[2]White, R. M., "Elastic Wave Generation by Electron Bombardment or Electromagnetic Wave Absorption," *Journal of Applied Physics*, Vol. 34, 1963, pp. 2123–2124.

[3]White, R. M., "Generation of Elastic Waves by Transient Surface Heating," *Journal of Applied Physics*, Vol. 34, 1963, pp. 3559–3567.

[4]Rykalin, N. N., Uglov, A. A., and Makarov, N. I., "Effects of Peak Frequency in a Laser Pulse on the Heating of Metal Sheets," *Soviet Physics — Doklady*, Vol. 12, 1967, pp. 644–646.

[5]Paek, U. C. and Gagliano, F. P., "Thermal Analysis of Laser Drilling Processes," *IEEE Journal of Quantum Electronics*, Vol. QE-8, 1972, pp. 112–119.

[6]Ready, J. F., *Effects of High Power Laser Radiation*, Academic, New York, 1971.

[7]Brugger, K., "Exact Solutions for Temperature Rise in a Laser Heated Slab, " *Journal of Applied Physics*, Vol. 43, 1972, pp. 577–583.

[8]Maydan, D., "Fast Modulator for Extraction of Internal Laser Power," *Journal of Applied Physics*, Vol. 41, 1970. pp. 1552–1559.

[9]Maydan, D., "Micromachining and Image Recording on Thin Films by Laser Beams," *Bell System Technical Journal*, Vol. 50, 1971, pp. 1761–1789.

[10]Modest, M. F. and Abakians, H., "Heat Conduction in a Moving Semi-Infinite Solid Subjected to Pulsed Laser Irradiation," *ASME Journal of Heat Transfer*, Vol. 108, 1986, pp. 597–601.

[11]Soodak, H., "Effects of Heat Transfer Between Gases and Solids," Ph.D. Thesis, Duke Univ., Durham, NC, 1943.

[12]Landau, H. G., "Heat Conduction in a Melting Solid," *Quarterly of Applied Mathematics*, Vol. 8, 1950, pp. 81–94.

[13]Dabby, F. W. and Paek, U. C., "High-Intensity Laser-Induced Vaporization and Explosion of Solid Material," *IEEE Journal of Quantum Electronics*, Vol. QE-8, 1972, pp. 106–111.

[14]von Allmen, M., "Laser Drilling Velocity in Metals," *Journal of Applied Physics*, Vol. 47, 1976, pp. 5460–5463.

[15]Modest, M. F. and Abakians, H., "Evaporative Cutting of a Semi-Infinite Body With a Moving CW Laser," *ASME Journal of Heat Transfer*, Vol. 108, 1986, pp. 602–607.

[16]Goodman, T. R., "Application of Integral Methods to Transient Nonlinear Heat Transfer," *Advances in Heat Transfer*, Vol. 1, edited by T. F. Irvine and J. P. Hartnet, Academic, New York, 1964, pp. 52–62.

[17]Biyikli, S. and Modest, M. F., "Beam Expansion and Focusing Effects on Evaporative Laser Cutting," *ASME Journal of Heat Transfer*, Vol. 110, 1988, pp. 529–532.

[18]Abakians, H. and Modest, M. F., "Evaporative Cutting of a Semi-Transparent Body with a Moving CW Laser," *ASME Journal of Heat Transfer*, Vol. 110, 1988, pp. 924–930.

[19]Brebbia, C. A., *Boundary Element Method for Engineers*, 2nd ed., Pentech, New York, 1978.

[20]Brebbia, C. A., Telles, J., and Wrobel, L., *Boundary Element Methods — Theory and Applications in Engineering*, Springer-Verlag, Berlin, 1983.

[21]Watson, J. O., "Advanced Implementation of the Boundary Element Method for Two- and Three-Dimensional Elasto-Statistics" *Developments in Boundary Element Methods*, edited by P. K.Bannerjee and R. Butterfield, Applied Science, London, 1979, Chap. III, pp. 31–63.